Activation of K_{ATP} Channels by Na/K pump in Isolated Cardiac Myocytes and Giant Membrane Patches

Anatolii Y. Kabakov
Department of Physiology, University of Texas, Southwestern Medical Center at Dallas, Dallas, Texas 75235 USA

ABSTRACT Strophanthidin inhibits K_{ATP} channels in 2,4-dinitrophenol-poisoned heart cells (Priebe et al., 1996). The current study shows that the Na/K pump interacts with K_{ATP} current ($I_{K\text{-}ATP}$) via submembrane ATP depletion in isolated giant membrane patches and in nonpoisoned guinea pig cardiac cells in whole-cell configuration. $I_{K\text{-}ATP}$ was inhibited by ATP, glibenclamide, or intracellular Cs^+. Na/K pump inactivation by substitution of cytoplasmic Na^+ for Li^+ or *N*-methylglucamine decreased both $I_{K\text{-}ATP}$ by 1/3 (1 mM ATP, zero calcium), and IC_{50} of ATP for $I_{K\text{-}ATP}$ (0.3 ± 0.1 mM) by 2/5. The Na^+/Li^+ replacement had no effect on $I_{K\text{-}ATP}$ at low pump activity ([ATP] ≤ 0.1 mM or 100 μM ouabain) or when $I_{K\text{-}ATP}$ was completely inhibited by 10 mM ATP. In whole-cell configuration, ouabain inhibited up to 60% of inwardly rectifying $I_{K\text{-}ATP}$ at 1 mM ATP in the pipette but not at 10 mM ATP and 10 mM phosphocreatine when $I_{K\text{-}ATP}$ was always blocked. However, mathematical simulation of giant-patch experiments revealed that only 20% of ATP depletion may be attributed to the ATP concentration gradient in the bulk solution, and the remaining 80% probably occurs in the submembrane space.

INTRODUCTION

How does the Na/K pump affect cellular excitability and the resting membrane potential? Activation of the pump produces outward pump current (Gadsby et al., 1993; Glitsch and Tappe, 1995) and causes changes of ionic and osmotic concentrations (Sperelakis, 1995). The resulting transmembrane osmotic water flux affects all the concentrations. In accordance with the Nernst-Plank approximation for passive currents the pump activation should always hyperpolarize the cell membrane at constant membrane ionic permeabilities (Goldman, 1943; Jakobsson, 1980; Kabakov, 1988a). However, at different ionic concentrations, the resting potential is described more accurately at constant membrane ionic conductivities, rather than the permeabilities (Hodgkin and Horowicz, 1959; Jaffe, 1974). In this case the dependence of the resting potential on the Na/K pump activity has a U-shaped form. In normal physiological conditions activation of the electrogenic Na/K pump will ultimately depolarize the cell membrane due to a larger effect on the sodium Nernst equilibrium potential relative to the potassium equilibrium potential (Kabakov, 1988a, 1994).

To describe the dependence of the resting potential on the Na/K pump activity more accurately we should incorporate effects of membrane potential and ionic concentrations on membrane ionic conductivities (Hille, 1992), as in the action potential models (DiFrancesco and Noble, 1985; Luo and Rudy, 1994; Saleet et al., 1998). However, all published mathematical models do not incorporate a direct effect (at constant membrane potential and ionic concentrations) of the pump on the membrane conductivities, although the Na/K pump apparently affects K_{ATP} channels via submembrane ATP depletion (Priebe et al., 1996). Here we would like to clarify the nature and quantitative parameters of this interaction.

Even direct physical interactions between the Na/K pump and some potassium channels or potassium channel modulators were proposed to explain inhibition of the tetraethylammonium-sensitive K^+ current by dihydroouabain in *Xenopus laevis* oocytes (Huang et al., 1995). However, other investigations confirm that the Na/K pump influences K_{ATP} channels via local ATP concentration changes. For example, activation of the Na/K pump in a renal proximal tubule by intracellular Na^+ resulted in both ATP depletion and an increase of relative K^+ conductance (Tsuchiya et al., 1992). Restoration of the ouabain-inhibited K^+ channel activity was observed after excision of a patch from a cell even with strophanthidin bathing the cytosolic face of the patch (Hurst et al., 1993). Blocking the pump with ouabain reduced the open probability of K_{ATP} channels in frog skin principal cells (Urbach et al., 1996). K_{ATP} channels in the cell-attached patch configuration were inhibited after strophanthidin was applied via the bath solution to metabolically poisoned heart cells (Priebe et al., 1996). Inhibition of the Na/K pump by ouabain led to inactivation of K_{ATP} channels in pancreatic β-cells (Tung et al., 1990; Grapengiesser et al., 1993). However, in all these experiments the pump-channel interaction was revealed in whole-cell or cell-attached patch configurations where control of intracellular ATP concentration and all cytoplasmic factors that might affect the K_{ATP} channels is not complete. The K^+ conductance may also rise not only as the result of ATP depletion (Noma, 1983; Benndorf et al., 1991, 1992; Deutsch and Weiss, 1993; Baghdady and Nichols, 1994) but also due to an increase of ADP (Lederer and Nichols, 1989), arachidonic acid (Chien et al., 1984; Kim and Claphan, 1989), and sodium (Kameyama et al., 1984; Ellis and Noireaud, 1987;

Received for publication 5 September 1997 and in final form 6 August 1998.

Address reprint requests to Dr. Anatolii Y. Kabakov, Department of Pharmacology and Therapeutics, University of Florida Medical College, Gainesville, FL 32610-0267. Tel.: 352-392-3257; Fax: 352-392-9696; E-mail: kabakov@nersp.nerdc.ufl.edu.

0006-3495/98/12/2858/10 $2.00

Tani and Neely, 1989). The only way to avoid confounding effects of cytoplasmic factors on the pump-channel interaction is to investigate it in isolated membrane patches. As the pump current cannot be measured in regular micro-patches due to low signal/noise ratio, the giant-patch configuration should be employed to measure both Na/K pump and K_{ATP} channel currents in the same isolated membrane.

The current study shows that Na/K pump activation leads to activation of the K_{ATP} channels via submembrane ATP depletion in isolated giant membrane patches where the control of both cytoplasmic and extracellular media is much more accurate. Although mathematical simulation of the phenomenon requires incorporation of a restricted diffusion space near the membrane (submembrane "fuzzy space"). The phenomenon was also demonstrated in nonpoisoned heart cells in whole-cell configuration with different ATP concentrations in the pipette.

MATERIALS AND METHODS

Preparation of isolated cardiac cells

Cardiac myocytes were isolated from female 300–450-g guinea pigs as described by Gadsby and Masakazu (1989). Animals were anesthetized by intraperitoneal injection of 3 ml of Nembutal (pentobarbital sodium, 50 mg/ml); 20 mg of aspirin and 10,000 U of heparin were also injected to hinder coagulation. The heart was excised, the aortic arch was cannulated, and retrograde coronary perfusion was begun, initially with normal Tyrode's solution containing 2 U/ml heparin to wash the blood, then with Ca-free Tyrode's until the heart stopped beating (~3 min), and then with Ca-free Tyrode's solution containing ~0.5 mg/ml collagenase (type 2, CLS-2, Worthington Biochemical Corp., NJ) until the exiting solution became "stringy" (~12 min). The collagenase was washed out of the heart with Ca-free Tyrode's solution (~8 min), followed by a solution containing 160 mM potassium. All solutions were oxygenated and warmed up to 38°C. The resulting partially digested heart was cut open and dissected into pieces approximately $3 \times 3 \times 2$ mm^3. Some of the pieces were stored 24 h at 4°C in the storage solution for giant-patch experiments. Other pieces were crudely minced and filtered of debris with fine nylon mesh with a 420-μm opening (Spectrum, CA) and then stored in the high K^+ solution at 4°C for the whole-cell experiments (Collins et al., 1992; Hilgemann, 1995a).

Electrophysiology

Axopatch 1C and 200A amplifiers were employed for both whole-cell and giant-patch (Hilgemann, 1995a) voltage clamp. The data were stored and analyzed on IBM-compatible computers as described previously (Kabakov and Hilgemann, 1995). The current was subsequently measured at the following holding potential levels (mV): 0, −30, −60, −90, −120, −150, −120, −90, −60, −30, 0, 30, 60, 90, 60, 30, and 0. All *I-V* curves presented here are the result of averaging of 4–10 individual experimental curves with error bars less than the sizes of the appropriate symbols. There was almost no hysteresis for increasing and decreasing voltage steps (see Figs. 1, 2 *B*, 3 *B*, 7, and 8).

An RC-5/25 chamber and CB-1N base (Warner Instrument Corp., CT) were used for the whole-cell experiments. All external solutions were warmed by passing through water-jacketed tubes (A-M Systems, WA). Temperature was monitored with a micro-thermistor bead (Fisher, number 15–077-11) positioned near the bottom of the chamber, close to the solution inflow, and it was maintained at 37°C while the temperature at the solution outflow was ~35°C (308 K).

Solutions

Modified Tyrode solution (containing (in mM) 145 NaCl, 5.4 KCl, 0.5 $MgCl_2$, 5.5 dextrose, 5 HEPES, and 1.8 $CaCl_2$) was, and the pH was adjusted to 7.4 with NaOH. In Ca-free Tyrode solution 1.8 mM $CaCl_2$ was replaced by 2.7 mM NaCl. The high K^+ solution contained (in mM) 20 taurine, 10 oxalic acid, 80 L-glutamic acid, 100 KOH, 10 KH_2PO_4, 10 HEPES, 25 KCl, 0.5 EGTA, 10 D-glucose, 5 pyruvic acid, 0.5 ATP, and 5 $MgSO_4$ and was adjusted to pH 7. 4 with KOH.

The maximal Na/K pump current in giant-patch and whole-cell configurations was first measured with potassium conductances blocked in potassium- and chloride-reduced solutions. The cytoplasmic solution had the following composition (mM): 100 NaOH, 30 CsOH, 100 DL-aspartic acid, 5 pyruvic acid, 20 tetraethylammonium chloride, 3 $MgCl_2$, 10 EGTA, 5.5 D-glucose, 10 HEPES, 10 ATP, 5 $Tris_2$-creatine phosphate; the pH was adjusted to 7.4 with MES. The extracellular solution contained (in mM) 145 *N*-methylglucamine (NMG), 5.4 KCl (or NMG to inactivate the pump in the whole-cell configuration), 4 $MgCl_2$, 1 EGTA, 10 HEPES, 6.6 HCl, and the pH was adjusted to 7.4 with MES. Fig. 1 shows the typical, nearly voltage-independent current-voltage (*I-V*) relation for the pump under these conditions.

To investigate interactions between the Na/K pump and K_{ATP} channels with maximal *I-V* response and maximal seal stability at 0 mV the same cytoplasmic and extracellular solutions were used in both giant-patch and whole-cell configurations (mM): 90 KCl, 20 NaCl, 40 NMG, 2 $MgCl_2$, 3 EGTA, and 10 HEPES; and the pH was adjusted to 7.4 with HCl and NMG. The 100 mM stock ATP solution contained (mM) 85 Mg-ATP, 15 Tris/ATP, and 30 HEPES, and pH was adjusted to 7.0 with NMG. ATP-free stock solution, used as a control, contained 130 mM HEPES with pH was adjusted to 7.0 with NMG. In all experiments 10% of each solution were replaced with a combination of the 100 mM ATP stock solution and ATP-free stock solution to get the appropriate cytoplasmic ATP concentration with the same concentrations of all major ions and the same osmolarity in all solutions. In the experiments with 10 or 100 μM glibenclamide the drug was added from 100 mM stock solution dissolved in dimethylsulfoxide. To inactivate the pump in these giant-patch experiments in the presence of ATP all Na^+ was replaced with NMG.

To monitor inward $I_{K\text{-}ATP}$ in the giant-patch configuration at 0 mV the cytoplasmic solution was replaced with a K^+-free solution (see Fig. 3) (mM): 150 LiCl, 10 HEPES, 3 EGTA, and 2 $MgCl_2$; pH was adjusted to 7.4 with HCl. The Na/K pump was activated by replacement of 20 mM LiCl with 20 mM NaCl.

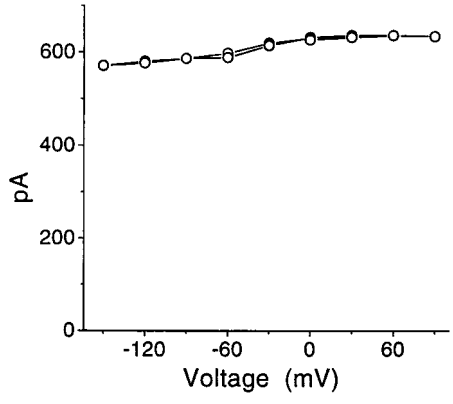

FIGURE 1 Extracellular K^+ elicits only outward pump current at all potentials when potassium channels are blocked by tetraethylammonium in the whole-cell configuration. The curve is the result of the subtraction of an average *I-V* curve in the absence of extracellular K^+ (substituted for NMG) from the curve in the presence of 5.4 mM extracellular K^+ ($[K]_i = [Na]_e = 0$; [ATP] = 10 mM) (number of *I-V* curves averaged, $n = 4$).

RESULTS

Na/K pump activation by cytoplasmic Na^+ activates $I_{K\text{-}ATP}$ in giant patches at 0.5 or 1 mM ATP but not at 0.1 mM or 10 mM ATP

In the first part of the study the interaction between the Na/K pump and K_{ATP} channels in the giant-patch configuration was investigated when the solutions on both sides of the membrane were identical (see Materials and Methods). At the beginning of an experiment, the inwardly rectifying current was usually rather small, but it became large after 0.5–10 mM ATP had been applied for ~1 min and removed. This activation of the K_{ATP} channels reflects the dual effect of ATP as an inhibitor and an activator of the channels (Findlay and Dunne, 1986; Nichols and Lederer, 1991; Furukawa et al., 1994) via phosphatidylinositol-4,5-bisphosphate generated by ATP from phosphatidylinositol (Hilgemann and Ball, 1996). The Na/K pump also has a slow phase of activation at the first application of ATP in giant patches (Hilgemann, 1995b; Friedrich et al., 1996). To have reproducible results, the channels and the pump were always preactivated with 10 mM ATP before each experiment.

In symmetrical solutions the Nernst potential for each ion is equal to zero. Therefore, the current elicited by ATP at 0 mV is only the pump current (Fig. 2 *A*). Here ATP-activated I_{pump} with K_{pump} equal to ~0.2 mM, which is in agreement with Friedrich et al. (1996). The inwardly rectifying $I_{K\text{-}ATP}$ current that is blocked by cytoplasmic Mg^{2+} at positive potentials (Horie et al., 1987; Lopatin et al., 1994) can also be revealed in these experiments when short voltage pulses were applied. Fig. 2 *B* shows current-voltage relations when the small background current was subtracted. The *I-V* curve of the background current was obtained when the K_{ATP} channels were completely blocked by 10 mM ATP and the pump was inactivated by replacement of cytoplasmic Na^+ for NMG. The Na^+/Ca^{2+} exchanger was not active in the presence of Na^+ due to absence of Ca^{2+} in all experimental solutions. In this experiment $I_{K\text{-}ATP}$ at −150 mV is inhibited by ATP with $IC_{50} \equiv K_{K\text{-}ATP} = 0.5$ mM, which is in agreement the with IC_{50} value found for $I_{K\text{-}ATP}$ by Kakei et al. (1985).

The inwardly rectified ATP-sensitive current in the absence of cytoplasmic Na^+ and Ca^{2+} on both sides of the membrane (see Materials and Methods) was identified as $I_{K\text{-}ATP}$ current. The $I_{K\text{-}ATP}$ current was not observed in the presence of 100 μM glibenclamide. In the presence of 10 μM glibenclamide the effect of 10 mM ATP application was insignificant (4 ± 3% of the total current). This is in agreement with Coetzee (1992), although Ripoll et al. (1993) reported that complete channel inhibition was not observed even at 300 μM glibenclamide. Therefore some researchers use 50 μM glibenclamide to block the K_{ATP} channels in the guinea pig ventricular myocytes (Docherty et al., 1997; Sato et al., 1995; Vanheel and de Hemptinne, 1992). Glibenclamide also inhibits a cardiac cAMP-activated Cl^- current with an IC_{50} of ~30 μM (Tominaga et al., 1995). Our solutions did not contain cAMP to activate

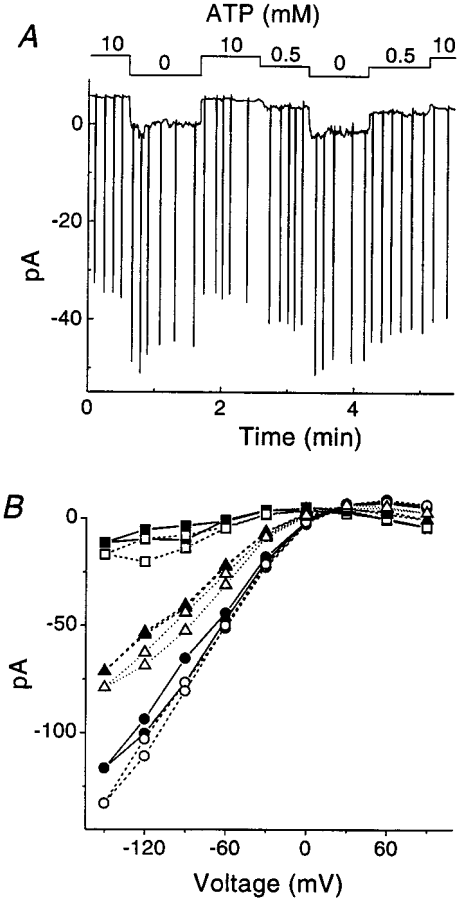

FIGURE 2 Reversible effect of ATP on the giant-patch currents. The contributing currents are mostly $I_{K\text{-}ATP}$ and I_{pump} when $[K]_i = [K]_e = 90$ mM and $[Na]_i = [Na]_e = 20$ mM. (*A*) The upper curve corresponds to the changes of cytoplasmic ATP during the experiment. The lower curve corresponds to total current at 0 mV, which represents I_{pump} as the equilibrium potentials for all ions are equal to zero in these conditions. Spikes correspond to the moments when the *I-V* measurements were made. (*B*) Average current-voltage relations presented at different ATP concentrations applied for the first time (*solid symbols*) or for the second time (*open symbols*) ($n = 5$). Squares correspond to 10 mM ATP, triangles to 0.5 mM, and circles to wash of ATP.

such a glibenclamide-sensitive chloride current. The $I_{K\text{-}ATP}$ was not contaminated with cAMP-activated Cl^- current as it was blocked by 20 mM cytoplasmic Cs^+. In addition, total ATP-independent current at −150 mV (I_{other}, which includes also the leak current) was less than 10% of $I_{K\text{-}ATP}$ (see Fig. 3 *B* and Appendix).

During an experiment the $I_{K\text{-}ATP}$ current is running down (Figs. 2 and 3) (Hilgemann and Ball, 1996). Therefore it was important to measure the *I-V* before and after the drug application. The effect of a drug on the *I-V* curve was determined with the following procedure for run-down currents as a difference between an average of *I-V* curves obtained during the drug application and average *I-V* curve obtained from two average *I-V* curves obtained before and after drug application.

The slope of the *I-V* curve at 10 mM ATP (Fig. 3 *B*) shows that total resistance was ~1 GΩ, but at positive

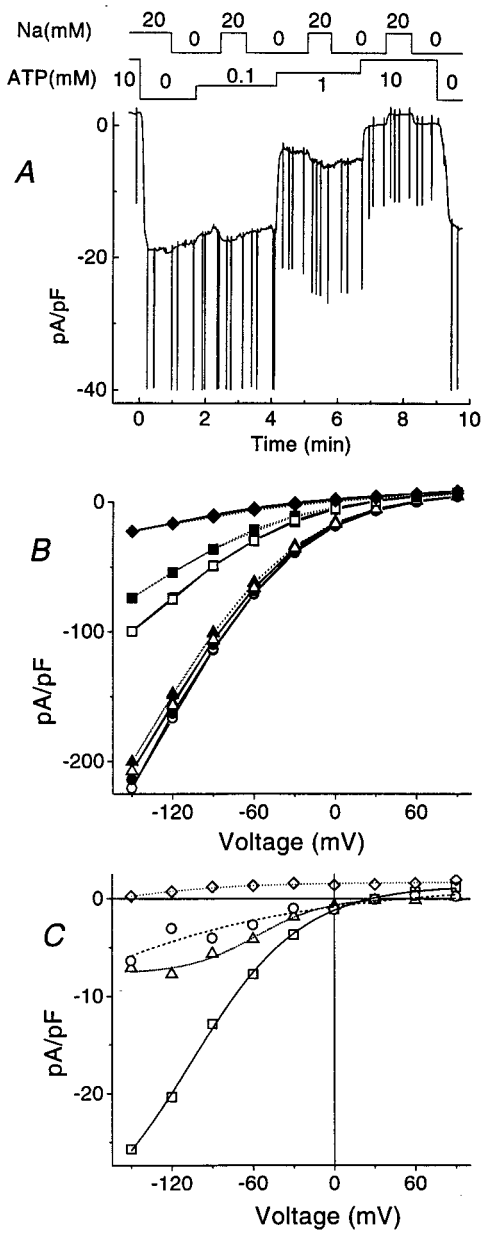

FIGURE 3 Effect of Na/K pump activation by intracellular Na^+ on $I_{K\text{-}ATP}$ at different ATP concentrations in K^+-free cytoplasmic solution. (*A*) The upper curve corresponds to 20 mM Na^+ applications (replacement for Li^+). Tne middle curve corresponds to different ATP concentrations from 0 to 10 mM. The lower curve is total current at 0 mV, which represents mostly the sum of I_{pump} and $I_{K\text{-}ATP}$ under these conditions. Spikes correspond to the moments of the *I-V* measurements. (*B*) Average *I-V* curves corresponding to Na^+ applications at different ATP concentrations ($n = 4$). Solid symbols, $[Na^+]_i = 0$ mM; open symbols, $[Na^+]_i = 20$ mM. ATP concentration in mM: diamonds, 10; squares, 1; triangles, 0.1; circles, wash of ATP. (*C*) Sodium-activated current at different ATP concentrations as a subtraction of corresponding curves in *B*. Maximal effect of the pump activation on $I_{K\text{-}ATP}$ occurs at 1 mM ATP (*squares*).

potentials, when the outward $I_{K\text{-}ATP} = 0$ ($[K^+]_i = 0$), the resistance rose up to 10 GΩ. Thus, the seal resistance in these experiments was higher than 10 GΩ.

The $I_{K\text{-}ATP}$ and I_{pump} at 0 mV were measured in K^+-free cytoplasmic solution containing 150 mM Li^+. In these experiments, when cytoplasmic sodium was not included, the inward current at 0 mV reflected mostly $I_{K\text{-}ATP}$ because it was inhibited by ATP (Fig. 3 *A*), by 10 μM glibenclamide, or by replacement of 20 mM cytoplasmic Li^+ with Cs^+. In the presence of 20 mM cytoplasmic Na^+ (replaced for Li^+) the inward $I_{K\text{-}ATP}$ was estimated as an ATP-sensitive current at −150 mV when I_{pump} was less than 1% of $I_{K\text{-}ATP}$. The outward I_{pump} was estimated as an ATP-sensitive current at +90 mV when the outward $I_{K\text{-}ATP} = 0$ ($[K^+]_i = 0$; Fig. 3).

Interaction between I_{pump} and $I_{K\text{-}ATP}$ was studied by applying and removing cytoplasmic Na^+ at different ATP concentrations. Fig. 3 *A* shows total current at 0 mV. Application of 20 mM Na^+ had almost no effect on the total current either at 0 mM or at 0.1 mM ATP. The sodium application caused prominent outward (pump) current with 10 mM ATP when $I_{K\text{-}ATP}$ was blocked, $\Delta I_{pump} > \Delta I_{K\text{-}ATP}$. However, application of intracellular sodium at 1 mM ATP elicited an inward current. This can be explained as a consequence of $I_{K\text{-}ATP}$ activation caused by Na/K pump depletion of submembrane ATP when $\Delta I_{pump} < \Delta I_{K\text{-}ATP}$.

The pump-channel interaction at 1 mM ATP is more evident at negative potentials (Fig. 3, *B* and *C*) where application of 20 mM Na^+ resulted in a large increase of the inward current caused by opening of the K_{ATP} channels. The effect was not observed in the presence of 100 μM ouabain in the pipette. When the bulk ATP concentration is smaller than $K_{K\text{-}ATP}$ and K_{pump} (e.g., 0.1 mM) the depletion of submembrane ATP is also small due to low pump activity. Therefore it has no significant effect on the K_{ATP} channels. The channels always remain unblocked at this ATP concentration.

At 5 or 10 mM bulk ATP, the submembrane ATP concentration is always high enough to block K-ATP channels completely even after ATP depletion. Thus, activation of the $I_{K\text{-}ATP}$ by the pump activation has biphasic dependence with respect to the bulk ATP concentration (Figs. 3 *C* and 6). The slight effect of sodium in the absence of ATP could result from traces of ATP (~0.5%) after a washout of 10 mM ATP from the same solution line.

Inhibition of the $I_{K\text{-}ATP}$ by bulk ATP in the presence and absence of intracellular Na^+ is shown in Fig. 4. Activation of the Na/K pump by intracellular Na^+ reversibly shifted $K_{K\text{-}ATP}$ (IC_{50}) from 0.5 to 0.8 mM. That is, at 0.8 mM bulk ATP, the pump activation reduced submembrane ATP concentration by ~0.3 mM. The average value of $K_{K\text{-}ATP}$ in the presence of Na^+ was 0.3 ± 0.1 mM (0.1–0.8 mM; $n = 9$). At 1 mM bulk ATP the pump-dependent submembrane ATP depletion was ~40% (0.4 mM).

Mathematical simulation of submembrane ATP depletion by the Na/K pump in the giant-patch configuration

The results of the giant-patch experiments are consistent with the idea that the pump-channel interaction occurs due

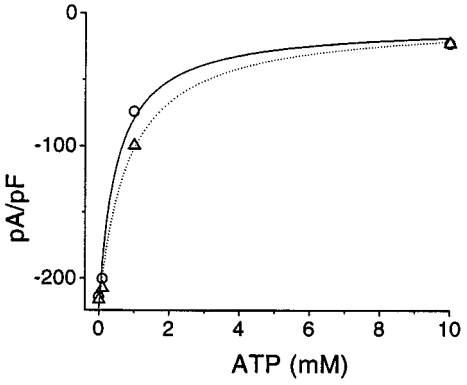

FIGURE 4 Na/K pump activation by Na^+ shifts the $I_{K\text{-}ATP}$ inhibition by ATP. The symbols represent total current at −150 mV in Fig. 3 *B* with (△) and without (○) intracellular Na^+. Curves correspond to the best fits of the equation: $I = I_{K\text{-}ATP,max}/(1 + [ATP]/K_{K\text{-}ATP}) + I_{other}$, with $I_{K\text{-}ATP,max}$ = 220 pA/pF, I_{other} = 6 pA/pF, and $K_{K\text{-}ATP}$ = 0.49 mM in the absence of Na^+ and $K_{K\text{-}ATP}$ = 0.80 mM in the presence of Na^+.

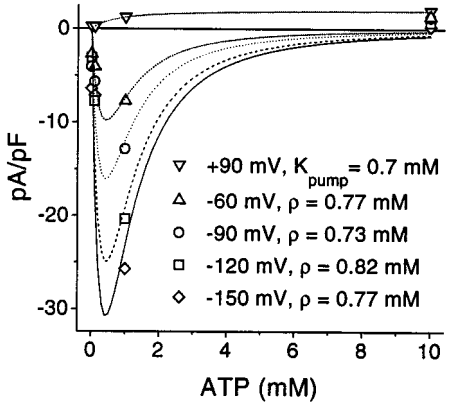

FIGURE 6 Effect of ATP on Na^+-activated pump-dependent component of $I_{K\text{-}ATP}$ at different membrane potentials. Symbols correspond to experimental data. Curves correspond to theoretical approximations. Upper curve at +90 mV corresponds to the best fit of the equation $I = I_{pump,max}/(1 + K_{pump}/[ATP])$ with $I_{pump,max}$ = 2.1 pA/pF. Lower curves correspond to the best fits of Eq. 10 with values of $I_{K\text{-}ATP,max}$ corresponding to appropriate potentials. The best-fit values of ρ are equal to 0.77, 0.73, 0.82, and 0.77 mM for the corresponding curves from the top (−60 mV) to the bottom (−150 mV).

to depletion of subsarcolemmal ATP. The question is whether the data could be explained by only ordinary ATP diffusion from the pipette tip to the giant-patch membrane or whether we need incorporation of ATP diffusion limitation in the submembrane space or some other factors. To consider this problem a mathematical simulation of the giant-patch experiments was performed (see Fig. 5 and Appendix).

The best fit of the pump-dependent component of $I_{K\text{-}ATP}$ ($I_{K\text{-}ATP,pump}$, determined by Eq. 10) to experimental data (Fig. 6) leads to an average value of maximal possible submembrane ATP depletion (ρ) equal to 0.77 mM for all negative potentials. But ρ calculated from Table 1 and experimental parameters for R_{tip} = 10 μm and $2\alpha = 30°$ is equal to 0.13 mM. If we take into account the ATP gradient outside of the pipette to support the same ATP flux we calculate ρ = 0.14 mM, which is still five times smaller than the best-fit value of ρ (0.77 mM) and two times smaller than the shift of $K_{K\text{-}ATP}$ caused by the pump ($K_{K\text{-}ATP,Li} - K_{K\text{-}ATP,Na}$ = 0.3 mM). The discrepancy may be related to diffusion limitation in the submembrane fuzzy space (Bielen et al., 1991; Carmeliet, 1992; Semb and Sejersted, 1996) as in a mature dendritic spine (Kabakov et al., 1998).

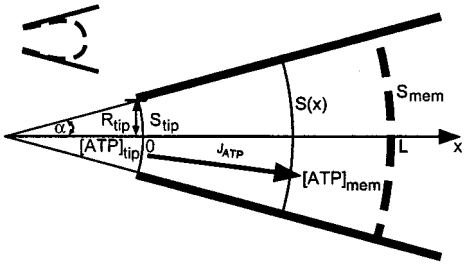

FIGURE 5 Schematic of the giant-patch membrane (*thick dashed line*) and the pipette tip (*thick solid line*). The system has symmetry with respect to the *x* axis. See symbols in Table 1. The inset in the top left of the figure shows a realistic shape of the giant patch.

In the steady-state approximation of submembrane sodium diffusion (Wendt-Gallitelli et al., 1993) the sodium diffusion coefficient D_{Na} in the fuzzy space is approximately equal to 1% of its value in water. But if we determine it as $D_{Na} = (\partial[Na]/\partial t)/(\partial^2[Na]/\partial x^2)$ from the submembrane sodium concentration gradients during systole and diastole in the same experiment, we calculate the value of D_{Na} as less than 0.001% of its value in water. The same fit as in Fig. 6 is possible with the normal value of D_{ATP} in the bulk solution, 3×10^{-10} m^2/s (Hubley et al., 1995) and a decrease of D_{ATP} in the submembrane space of 200-nm width to 0.023% of its normal value (i.e., to 7×10^{-14} m^2/s). This value of D_{ATP} is still significantly less than the value of D_{ATP} in aqueous pores, $(1.6–3.3) \times 10^{-11}$ m^2/s (Rostovtseva and Bezrukov, 1998). Nonetheless we can accurately simulate the pump-channel interaction in the giant-patch experiments with this significant ATP diffusion limitation in submembrane space, although other possible factors are mentioned in the Discussion.

Ouabain decreases $I_{K\text{-}ATP}$ in whole-cell configuration at 1 or 3 mM ATP in the pipette but not at 10 mM ATP with 10 mM creatine phosphate

If the pump-channel interaction occurs through the ATP depletion then pump activity should not have an effect at high ATP concentrations when even depleted ATP is high enough to block K_{ATP} channels completely in the whole-cell configuration.

Fig. 7 shows that application of 50 μM extracellular ouabain reduces the dominant inwardly rectifying current by 60% in the whole-cell configuration with 3 mM ATP in the pipette and when intracellular and extracellular ion

TABLE 1 Description of symbols

Symbol	Meaning of the symbol (all units are in SI format)
$[ATP]_{mem}$	ATP concentration at the membrane
$[ATP]_{tip}$	ATP concentration at the pipette tip
$ATP(x)$	Average ATP concentration on the segment of an intermediate spherical surface as a function of x
$[Cl]_e$	Extracellular concentration of chloride
$[Cl]_i$	Intracellular concentration of chloride
C_{mem}	Capacitance of membrane patch
c_{spec}	Specific membrane capacitance = 10^{-2} F/m^2
D_{ATP}	ATP diffusion coefficient = 3×10^{-10} m^2/s (Hubley et al., 1995)
F	Faraday constant = 96.5 coul/mmol
g_K	Potassium conductivity of cell membrane
g_{Na}	Sodium conductivity of cell membrane
g_{Cl}	Chloride conductivity of cell membrane
$I_{K\text{-}ATP}$	ATP-sensitive K^+ current
$I_{K\text{-}ATP,max}$	Maximal $I_{K\text{-}ATP}$
$I_{K\text{-}ATP,pump}$	Na/K pump-dependent component of $I_{K\text{-}ATP}$
I_{other}	All currents except $I_{K\text{-}ATP}$ and I_{pump} (such as leak current)
I_{pump}	Na/K pump current
$I_{pump,max}$	Maximal I_{pump}
$J_{ATP}(x)$	ATP flux as a function of distance x
$J_{ATP,mem}$	Submembrane ATP flux = $J_{ATP}(L)$
$[K]_e$	Extracellular concentration of potassium
$[K]_i$	Intracellular concentration of potassium
$K_{K\text{-}ATP}$	ATP concentration corresponding to half-maximal inhibition of the K_{ATP} channels (IC_{50})
$K_{K\text{-}ATP,Li}$	$K_{K\text{-}ATP}$ when intracellular Na was replaced by Li
K_{pump}	Apparent dissociation constant of the ATP binding with the Na/K pump
L	Distance from the pipette tip to the membrane $\equiv (S_{mem}/\beta)^{1/2} - R_{tip}/\sin(\alpha)$
M_e	Extracellular osmotic concentration
$[Na]_e$	Extracellular concentration of sodium
$[Na]_i$	Intracellular concentration of sodium
R	Gas constant = 8.314 J mol^{-1} K^{-1}
R_{tip}	Internal radius of the pipette tip
r	Stoichiometry of Na/K pump = 3/2
S_{mem}	Area of the giant-patch membrane (Fig. 5)
S_{tip}	Area of a segment of the spherical surface at the pipette tip
$S(x)$	Area of a segment of an intermediate spherical surface as a function of x
T	Thermodynamic temperature = 309°K
V	Membrane potential
V^i	Inversion potential
x	Distance from S_{tip} to $S(x)$ on the axis x (Fig. 5)
α	Angle 2α is the pipette tip angle (Fig. 5)
β	Constant = $2\pi(1 - \cos(\alpha))$
θ	Constant = $(N - Q)/Q$; where N is total number of soluble intracellular impermeant neutral molecules and soluble impermeant ions, and Q is the number of corresponding to the total intracellular impermeant charge, which is counted in elementary charges (-1.6×10^{-19} C)
λ	Constant = $(S_{mem} - S^{1/2}{}_{tip} S_{mem}{}^{1/2})/(\beta\, S_{tip})^{1/2}$
ρ	Constant = $I_{pump,max} c_{spec} \lambda/(D_{ATP} C_{mem} F)$, corresponds to maximal ATP depletion at maximal pump activity

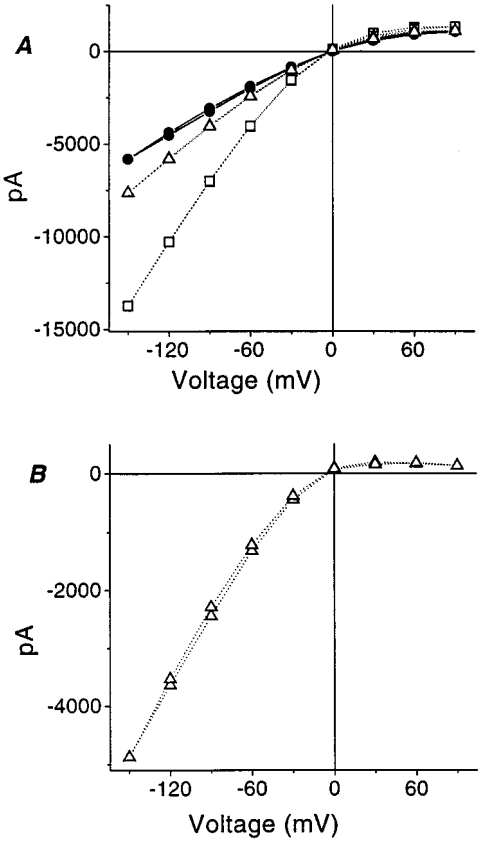

FIGURE 7 Ouabain inhibits $I_{K\text{-}ATP}$ in the presence of 3 mM ATP in the pipette in the whole-cell configuration (R_{tip} = 1 μm). (*A*) *I-V* relationships of the whole-cell current were obtained before ouabain application (□) and then in the presence of 50 μM extracellular ouabain (●) and after wash of ouabain (△) (n = 5). (*B*) The ouabain-sensitive component of the current is presented as a subtraction of the current in the presence of 50 μM extracellular ouabain from the average current in the absence of ouabain. Intracellular and extracellular solutions are symmetrical with 90 mM KCl and 20 mM NaCl.

concentrations are identical. A similar effect was found at 1 mM ATP (not shown). The effect of ouabain was partially reversible (n = 12). The effect was larger at a smaller internal diameter of the pipette tip (~1 μm) where ATP diffusion from the pipette to the cell membrane was more restricted. The current reversed at 0 mV as was expected. The effect was not observed in the presence of 100 or 10 μM extracellular glibenclamide. Probably at 1 or 3 mM ATP in the pipette the Na/K pump activation can reduce submembrane ATP concentration from its unknown level (because we do not know rates of cytoplasmic ATP production and consumption in our experiments) down to 0.1–0.5 mM, which causes activation of $I_{K\text{-}ATP}$ (Tung et al., 1990; Grapengiesser et al., 1993; Priebe et al., 1996).

However, at 10 mM ATP and 10 mM creatine phosphate in the pipette with large internal diameter of the tip (~4 μm), application of 50 μM ouabain had an effect on outward pump current but not on the inwardly rectifying current (Fig. 8). Under these conditions K_{ATP} channels are always blocked by ATP because depletion of submembrane ATP by the active pump is not sufficient to decrease the submembrane ATP concentration close to $K_{K\text{-}ATP}$ (from 0.114 mM to 0.5 mM ATP; Nichols et al., 1991; Kakei et al., 1985; Furukawa et al., 1994). The ouabain-sensitive current at high ATP (Fig. 8) is I_{pump}, which is similar to I_{pump} activated by external potassium in the presence of tetraethylammonium chloride (Fig. 1).

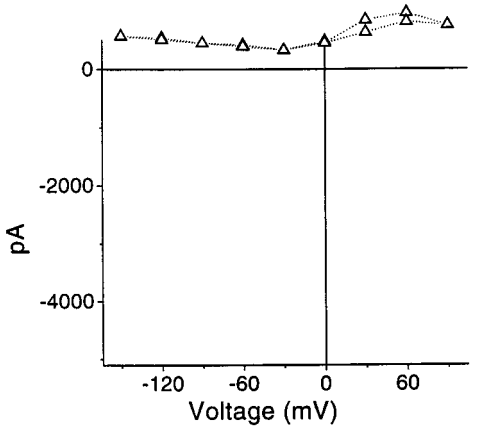

FIGURE 8 Ouabain has no effect on the inwardly rectifying $I_{K\text{-}ATP}$ in the presence of 10 mM ATP and 10 mM creatine phosphate in the pipette (R_{tip} = 2 μm) in the whole-cell configuration because even partially depleted submembrane ATP is sufficient to block K_{ATP} channels. The ouabain-sensitive component of the current is presented as a subtraction of the current in the presence of 50 μM extracellular ouabain from the average current in the absence of ouabain (as in Fig. 7 *B*) (n = 4). The curve represents only the outward pump current. Intracellular and extracellular solutions are symmetrical with 90 mM KCl and 20 mM NaCl.

DISCUSSION

The pump-channel interaction

This study shows that the pump-channel interaction exists in isolated membranes that are free of any unidentified cytoplasmic factors (see Introduction). In the whole-cell configuration the ATP hydrolysis by the Na/K pump can cause activation of K_{ATP} channels via ATP depletion in the submembrane space (thus relieving the ATP-dependent block) even without poisoning cells with 2,4-dinitrophenol (Priebe et al., 1996).

The Na/K pump activation in the giant-patch configuration by intracellular Na^+ has almost no effect on $I_{K\text{-}ATP}$ at bulk ATP concentrations lower than 0.1 mM (lower than $K_{K\text{-}ATP}$ and K_{pump}). The pump activation also has no effect on $I_{K\text{-}ATP}$ at bulk ATP concentrations higher than 5 mM because submembrane ATP depletion by the pump (less than 1 mM) is not sufficient to activate K_{ATP} channels (Figs. 3 and 4). However, the pump activation significantly activates $I_{K\text{-}ATP}$ at 0.5 or 1 mM ATP in the bulk solution (Figs. 3 and 4) because the depletion of submembrane ATP (apparently by 0.2–0.4 mM) occurs in the range of $K_{K\text{-}ATP}$ (Figs. 4 and 6).

The effect of the Na/K pump activation on K_{ATP} channels is larger in the whole-cell configuration than in the giant patch. This is expected if the effect is related to ATP diffusion and depletion. Diffusion distances in giant patches are shorter than in the whole cell where ATP must diffuse from the pipette into the myocyte to provide ATP to the pump. However, high ATP and creatine phosphate concentrations in the pipette would overcome the depleting effect of the pump on K_{ATP} channels. As this is the case, the diffusion of ATP from the pipette is a major source of ATP for the Na/K pump in the whole-cell experiments. It is less clear what to expect in the case of the cardiac cell that produces its own ATP. But even in this case depletion will occur because of the existence of the diffusion distance between mitochondria and cell membrane.

In the giant-patch experiments the half-maximal inhibition of the potassium current by ATP varied from 0.1 to 0.8 mM (0.3 $\pm$ 0.1 mM) in the presence of cytoplasmic Na^+. This variability is in agreement with the literature (Nichols et al., 1991; Takano and Noma, 1993; Findlay and Dunne, 1986; Furukawa et al., 1994). The variability may be related to differences in pipette and membrane geometries, and in total membrane ATPase activity, leading to different degrees of ATP depletion. The value of $K_{K\text{-}ATP}$ also depends on duration and concentration of ATP preapplication (Findlay and Dunne, 1986; Furukawa et al., 1994; Hilgemann and Ball, 1996).

The best fits of the pump-dependent component of $I_{K\text{-}ATP}$ ($I_{K\text{-}ATP,pump}$ in Eq. 10) at different cytoplasmic ATP concentrations and all negative membrane potentials in the experiment shown in Figs. 3 and 4 have almost the same value of the fitting parameter ρ (ATP depletion at maximal pump activity) of ~0.77 mM (Fig. 6). The value of ρ is five times smaller when calculated from the experimental parameters and its determination in Table 1 without submembrane diffusion limitation. The discrepancy might be due to several factors: 1) lower ATP diffusion coefficient in the submembrane space than that in water, 2) overestimation of the pipette tip area that is available for free ATP diffusion, 3) existence of sodium-independent phosphorylation at the membrane and consequently some sodium-independent submembrane ATP depletion, 4) effect of ADP (Lederer and Nichols, 1989) and sodium (Tani and Neely, 1989; Ellis and Noireaud, 1987; Kameyama et al., 1984) on $I_{K\text{-}ATP}$, and 5) geometrical and kinetic simplifications made in the mathematical simulation. However, the ATP diffusion limitation in the submembrane space is sufficient to simulate the pump-channel interaction accurately (Fig. 6).

The Na/K pump and the resting membrane potential

The dependence of the resting potential on the Na/K pump activity can still be described analytically by Eq. 1 (Kabakov, 1994) even if the pump-channel interaction is taken into account:

$$V = \frac{RT}{F}\ln(-M_e + (M_e^2 + 4\theta(\theta+2)[Cl]_e([K]_e e^{-2I_{pump}F/g_K RT} + [Na]_e e^{+3I_{pump}F/g_{Na}RT}))^{1/2})/(2\theta[Cl]_e), \quad (1)$$

where g_K is an analytical function (such as the one described by Eqs. 9 and 10) of several variables, including Na/K pump activity (I_{pump}), cell geometry, cell ATP production and consumption with their locations in the cell, average density of K_{ATP} channels with appropriate voltage-

independent conductivity (at the physiological range of the resting potential, i.e., $g_{K\text{-}ATP,max}$ in the absence of ATP), which depends only on ATP concentration with appropriate $K_{K\text{-}ATP}$.

The relation between the membrane potential and the Na/K pump activity is complex and depends on the nature of the pump activation (or inactivation). The approach described here is more adequate for the steady-state conditions when pump inactivation is caused by a pump-specific inhibitor, i.e., ouabain. However, the dependence of the potential on the pump activity would be different if the pump was inactivated, for example, by a decrease in the intracellular ATP during ischemia (Kabakov, 1988b). In this case we will be able to find only a numerical solution but not the analytical one.

Submembrane ATP diffusion limitation

Mathematical simulation of the pump-channel interaction requires a submembrane ATP diffusion limitation that is in agreement with submembrane ion diffusion limitations used to explain other electrophysiological phenomena (Bielen et al., 1991; Carmeliet, 1992; Semb and Sejersted, 1996). For sodium this limitation is proven by direct measurements (Wendt-Gallitelli et al., 1993). However, the restriction of ATP diffusion requires additional investigations.

APPENDIX

Mathematical simulation of the pump-dependent component of $I_{K\text{-}ATP}$ ($I_{K\text{-}ATP,pump}$) at different ATP concentrations in the giant-patch experiments

The ATP diffusion caused by submembrane ATP depletion has been approximated as a steady-state radial ATP flux from a segment of spherical surface S_{tip} at the pipette tip to a segment of spherical surface S_{mem} of the membrane where both spherical surfaces have the same center (Fig. 5; Table 1). The ATP flux through an intermediate spherical surface $S(x)$ located between S_{tip} and S_{mem} was determined from Fick's law as a function of distance x from S_{tip} to $S(x)$:

$$J_{ATP}(x) = -D_{ATP}\frac{\partial[\mathrm{ATP}(x)]}{\partial x} \tag{2}$$

In the steady state we have

$$J_{ATP}(x)/J_{ATP,mem} = S_{mem}/S(x) \tag{3}$$

The value of ATP flux at the membrane ($J_{ATP,mem}$) is determined by I_{pump} assuming that one ATP molecule is consumed for one net outward charge movement:

$$J_{ATP,mem} = \frac{I_{pump}c_{spec}}{C_{mem}F} \tag{4}$$

The area of an intermediate $S(x)$ can be expressed as a function of x:

$$S(x) = \beta(R_{tip}/\sin(\alpha) + x)^2 = S_{tip}(1 + x(\beta/S_{tip})^{1/2})^2 \tag{5}$$

ATP depletion at the membrane with respect to ATP concentration at the pipette tip can be calculated as an integral of Eq. 2 from 0 to L with appropriate substitutions incorporating Eqs. 3 and 5:

$$[\mathrm{ATP}]_{mem} - [\mathrm{ATP}]_{tip} = \int_0^L \frac{-J_{ATP,mem}S_{mem}\,dx}{D_{ATP}S_{tip}(1 + x(\beta/S_{tip})^{1/2})^2}$$

That is,

$$[\mathrm{ATP}]_{mem} = [\mathrm{ATP}]_{tip} - \lambda\frac{J_{ATP,mem}}{D_{ATP}} \tag{6}$$

and

$$J_{ATP,mem} = \frac{D_{ATP}}{\lambda}([\mathrm{ATP}]_{tip} - [\mathrm{ATP}]_{mem}), \tag{7}$$

where λ is a constant determined only by the geometry of the pipette and the membrane patch (see Table 1).

The dependence of the pump current on the submembrane ATP concentration was approximated as

$$I_{pump} = I_{pump,max}\frac{1}{1 + \dfrac{K_{pump}}{[\mathrm{ATP}]_{mem}}}$$

Substituting this expression into Eq. 4 yields

$$J_{ATP,mem} = \frac{I_{pump,max}c_{spec}[\mathrm{ATP}]_{mem}}{C_{mem}F([\mathrm{ATP}]_{mem} + K_{pump})} \tag{8}$$

Now we can find the submembrane ATP concentration as a function of ATP concentration at the pipette tip by solving a list of simultaneous Eqs. 7 and 8:

$$[\mathrm{ATP}]_{mem} = ([\mathrm{ATP}]_{tip} - K_{pump} - \rho + (([\mathrm{ATP}]_{tip} - K_{pump} - \rho)^2 + 4[\mathrm{ATP}]_{tip}K_{pump})^{1/2})/2, \tag{9}$$

where ρ is a constant that corresponds to ATP depletion ($[\mathrm{ATP}]_{tip} - [\mathrm{ATP}]_{mem}$) at maximal pump activity and depends on the patch geometry.

Inhibition of $I_{K\text{-}ATP}$ by ATP was approximated as

$$I_{K\text{-}ATP} = I_{K\text{-}ATP,max}\frac{1}{1 + \dfrac{[\mathrm{ATP}]_{mem}}{K_{K\text{-}ATP}}}$$

and total patch current as

$$I_{total} = I_{K\text{-}ATP} + I_{pump} + I_{other}$$

Some parameters of theoretical patch can be found by fitting of I_{total} to experimental data. $I_{K\text{-}ATP}$ contributes more than 90% to I_{total} at negative potentials (Fig. 3 *B*). From data presented in Figs. 3 and 4 we can find that at −150 mV I_{other} = 6 pA/pF, $I_{K\text{-}ATP,max}$ = 220 pA/pF; in the absence of cytoplasmic Na^+ (substituted for Li^+), $K_{K\text{-}ATP,Li}$ = 0.49 mM; and in the presence of 20 mM cytoplasmic Na^+, $K_{K\text{-}ATP,Na}$ = 0.80 mM (Fig. 4).

As outward $I_{K\text{-}ATP,max} = 0$ at +90 mV ($[K^+]_i = 0$) we can approximate that the ATP-sensitive outward current stimulated by 20 mM cytoplasmic Na^+ at +90 mV is the pump current (Fig. 3 *C*) with K_{pump} = 0.7 mM and $I_{pump,max}$ = 2.1 pA/pF × 10 pF = 21 pA (here C_{mem} = 10 pF).

Now we can find $I_{K\text{-}ATP,pump}$ at different $[\mathrm{ATP}]_{tip}$ in the negative potential range. This component of $I_{K\text{-}ATP}$ is equal to the difference between $I_{K\text{-}ATP}$ currents in the presence and absence of the submembrane

ATP depletion by the pump:

$$I_{\text{K-ATP,pump}} = I_{\text{K-ATP,max}} \frac{1}{1 + \frac{[\text{ATP}]_{\text{mem}}}{K_{\text{K-ATP}}}} - I_{\text{K-ATP,max}} \frac{1}{1 + \frac{[\text{ATP}]_{\text{tip}}}{K_{\text{K-ATP}}}}, \quad (10)$$

where $[\text{ATP}]_{\text{mem}}$ must be substituted with the Eq. 9 as a function of ρ, $[\text{ATP}]_{\text{tip}}$, and K_{pump}.

I thank Dr. Donald W. Hilgemann for generous permission to conduct these experiments in his laboratory and for valuable discussions, Dr. David C. Gadsby, Dr. Neal Shepherd, Peter Hoff, and Athanasios Dousmanis for instructing me in the use of the whole-cell technique and in cell preparation, Siyi Feng for technical assistance, Dr. Nicholas Sperelakis and Dr. Yoram Rudy for encouragement, and Dr. Colin G. Nichols, Dr. Anatoli Lopatin, Dr. David C. Gadsby, Dr. Robert S. Reneman, Nikolas B. Karkanias, and reviewers of the Biophysical Journal for critical remarks.

This work was supported by National Institutes of Health grant 1RO1HI51323–01, a grant-in-aid from the American Heart Association (95014830 to Dr. Donald W. Hilgemann), and by the spirit of curiosity.

REFERENCES

Baghdady, R., and C. Nichols. 1994. ATP sensitive potassium channels and ischemic heart disease. *Cardiovasc. Res.* 28:135–136.

Benndorf, K., G. Bollmann, M. Friedrich, and H. Hirche. 1992. Anoxia induces time-independent K^+ current through K_{ATP} channels in isolated heart cells of the guinea pig. *J. Physiol. (Lond.).* 454:339–357.

Benndorf, K., M. Friedrich, and H. Hirche. 1991. Anoxia opens ATP regulated K channels in isolated heart cells of the guinea pig. *Pflugers Arch.* 419:108–110.

Bielen, F. V., H. G. Glitsch, and F. Verdonck. 1991. Changes of the subsarcolemmal Na^+ concentration in internally perfused cardiac cells. *Biochim. Biophys. Acta.* 1065:269–271.

Carmeliet, E. 1992. A fuzzy subsarcolemmal space for intracellular Na^+ in cardiac cells? *Cardiovasc. Res.* 26:433–442.

Chien, K. R., A. Han, A. Sen, L. M. Buja, and J. T. Willerson. 1984. Accumulation of unesterified arachidonic acid in ischemic canine myocardium. *Circ. Res.* 54:313–322.

Coetzee, W. A. 1992. Regulation of ATP sensitive potassium channel of isolated guinea pig ventricular myocytes by sarcolemmal monocarboxylate transport. *Cardiovasc. Res.* 26:1077–1086.

Collins, A., A. V. Somlyo, and D. W. Hilgemann. 1992. The giant cardiac patch method: stimulation of outward Na^+-Ca^{2+} exchange current by MgATP. *J. Physiol. (Lond.).* 454:27–57.

Deutsch, N., and J. N. Weiss. 1993. ATP-sensitive K^+ channel modulation by metabolic inhibition in isolated guinea-pig ventricular myocytes. *J. Physiol. (Lond.).* 465:163–179.

DiFrancesco, D., and D. Noble. 1985. A model of cardiac electrical activity incorporating ionic pumps and concentration changes. *Philos. Trans. R. Soc. Lond.* 307:353–398.

Docherty, J. C., H. E. Gunter, B. Kuzio, L. Shoemaker, L. Yang, and R. Deslauriers. 1997. Effects of cromakalim and glibenclamide on myocardial high energy phosphates and intracellular pH during ischemia-reperfusion: ^{31}P NMR studies. *J. Mol. Cell. Cardiol.* 29:1665–1673.

Ellis, D., and J. Noireaud. 1987. Intracellular pH in sheep Purkinje fibres and ferret papillary muscles during hypoxia and recovery. *J. Physiol. (Lond.).* 383:125–141.

Findlay, I., and M. J. Dunne. 1986. ATP Maintains ATP-inhibited K^+ channels in an operational state. *Pfugers Arch.* 407:238–240.

Friedrich, T., Bamberg, E., and Nagel, G. 1996. Na^+,K^+-ATPase pump currents in giant excised patches activated by an ATP concentration jump. *Biophys. J.* 71:2486–2500.

Furukawa, T., L. Virág, N. Furukawa, T. Sawanobori, and M. Hiraoka. 1994. Mechanism for reactivation of the ATP-sensitive K^+ channel by MgATP complexes in guinea-pig ventricular myocytes. *J. Physiol. (Lond.).* 479:95–107.

Gadsby, D. C., and N. Masakazu. 1989. Steady-state current-voltage relationship of the Na/K pump in guinea pig ventricular myocytes. *J. Gen. Physiol.* 94:511–537.

Gadsby, D. C., R. F. Rakowski, and P. De-Weer. 1993. Extracellular access to the Na/K pump: pathway similar to ion channel. *Science.* 260: 100–103.

Glitsch, H. G., and A. Tappe. 1995. Change of Na^+ pump current reversal potential in sheep cardiac Purkinje cells with varying free energy of ATP hydrolysis. *J. Physiol. (Lond.).* 484:605–616.

Goldman, D. E. 1943. Potential, impedance, and rectification in membranes. *J. Gen. Physiol.* 27:37–60.

Grapengiesser, E., A. Berts, S. Saha, P.-E. Lund, E. Gylfe, and B. Hellman. 1993. Dual effect of Na/K pump inhibition on cytoplasmic Ca^{2+} oscillations in pancreatic β-cells. *Arch. Biochem. Biophys.* 300:372–377.

Hodgkin, A. L., and P. Horowicz. 1959. The influence of potassium and chloride ions on the membrane potential of single muscle fibres. *J. Physiol. (Lond.).* 148:127–160.

Hilgemann, D. W. 1995a. The giant membrane patch. *In* Single-Channel Recording. B. Sakmann and E. Neher, editors. Plenum Press, New York. 307–327.

Hilgemann, D. W. 1995b. Slow activation of Na/K pump on first application of ATP in giant patches: comparison to Na/Ca exchange. *Biophys. J.* 68:A307

Hilgemann, D. W., and R. Ball. 1996. Regulation of cardiac Na^+,Ca^{2+} exchange and K_{ATP} potassium channels by PIP_2. *Science.* 273:956–959.

Hille, B. 1992. Ionic channels of excitable membranes. Sunderland, MA.

Horie, M., H. Irisawa, and A. Noma. 1987. Voltage-dependent magnesium block of adenosine-triphosphate-sensitive potassium channel in guinea-pig ventricle cells. *J. Physiol. (Lond.).* 387:251–272.

Huang, H., H. St.-Jean, M. J. Coady, and J. Y. Lapointe. 1995. Evidence for coupling between Na^+ pump activity and TEA-sensitive K^+ current in *Xenopus laevis* oocytes. *J. Membr. Biol.* 143:29–35.

Hubley, M. J., R. C. Rosanske, and T. S. Moerland. 1995. Diffusion coefficients of ATP and creatine phosphate in isolated muscle: pulsed gradient ^{31}P NMR of small biological samples. *NMR Biomed.* 8:72–78.

Hurst, A. M., J. S. Beck, R. Laprade, and J. Y. Lapointe. 1993. Na^+ pump inhibition downregulates an ATP-sensitive K^+ channel in rabbit proximal convoluted tubule. *Am. J. Physiol.* 264:F760–F764.

Jaffe, L. F. 1974. The interpretation of voltage-concentration relations. *J. Theor. Biol.* 48:11–18.

Jakobsson, E. 1980. Interaction of cell volume, membrane potential, and membrane transport parameters. *Am. J. Physiol.* 238:C196–C206.

Kabakov, A. Y. 1988a. Hyperpolarization of the cell membrane on inactivation of Na,K-ATPase. *Biophysics.* 33:320–327.

Kabakov, A. Y. 1988b. Analysis of equivalent electric circuit of a hepatocyte in conditions of arrest and restoration of blood flow. *Biophysics.* 33:890–896.

Kabakov, A. Y. 1994. The resting potential equations incorporating ionic pumps and osmotic concentration. *J. Theor. Biol.* 169:51–64.

Kabakov, A. Y., and D. W. Hilgemann. 1995. Modulation of Na^+,Ca^{2+} exchange current by EGTA calcium buffering in giant cardiac membrane patches. *Biochim. Biophys. Acta.* 1240:142–148.

Kabakov, A. Y., B. N. Karkanias, R. H. Lenox, and R. L. Papke. 1998. Synapse specific accumulation of lithium in intracellular microdomains: a model for uncoupling coincidence detection in the brain. *Synapse.* 28:271–279.

Kakei, M., A. Noma, and T. Shibasaki. 1985. Properties of adenosine-triphosphate-regulated potassium channels in guinea-pig ventricular cells. *J. Physiol. (Lond.).* 363:441–462.

Kameyama, M., M. Kakei, R. Sato, T. Shibasaki, H. Matsuda, and H. Irisawa. 1984. Intracellular Na^+ activates a K^+ channel in mammalian cardiac cells. *Nature.* 309:354–356.

Kim, D., and D. E. Claphan. 1989. Potassium channels in cardiac cells activated by arachidonic acid and phospholipids. *Science.* 244: 1174–1176.

Lederer, W. J., and C. G. Nichols. 1989. Nucleotide modulation of the activity of rat heart ATP-sensitive K^+ channels in isolated membrane patches. *J. Physiol. (Lond.).* 419:193–211.

Lopatin, A. N., E. N. Makhina, and C. G. Nichols. 1994. Potassium channel block by cytoplasmic polyamines as the mechanism of intrinsic rectification. *Nature.* 372:366–369.

Luo, C. H., and Y. Rudy. 1994. Adynamic model of the cardiac ventricular action potential. I. Simulations of ionic currents and concentration changes. *Circ. Res.* 74:1071–1096.

Nichols, C. G., and W. J. Lederer. 1991. The mechanism of K_{ATP} channel inhibition by ATP. *J. Gen. Physiol.* 97:1095–1098.

Nichols, C. G., C. Ripoll, and W. J. Lederer. 1991. ATP-sensitive potassium channel modulation of the guinea pig ventricular action potential and contraction. *Circ. Res.* 68:280–287.

Noma, A. 1983. ATP-regulated K^+ channels in cardiac muscle. *Nature.* 305:147–148.

Priebe, L., M. Friedrich, and K. Benndorf. 1996. Functional interaction between K_{ATP} channels and the Na^+-K^+ pump in metabolically inhibited heart cells of the guinea pig. *J. Physiol. (Lond.).* 492:405–417.

Ripoll, C., W. J. Lederer, and C. G. Nichols. 1993. On the mechanism of inhibition of K_{ATP} channels in rat ventricular myocytes. *J. Cardiovasc. Electrophysiol.* 4:38–47.

Rostovtseva, T. K., and S. M. Bezrukov. 1998. ATP transport through a single mitochondrial channel, VDAC, studied by current fluctuation analysis. *Biophys. J.* 74:2365–2373.

Saleet, M. J., J. J. Rice, and R. L. Winslow. 1998. Cardiac Ca^{2+} dynamics: the roles of ryanodine receptors adaptation and sarcoplasmic reticulum load. *Biophys. J.* 74:1149–1168.

Sato, T., S. Shigematsu, and M. Arita. 1995. Mexiletine-induced shortening of the action potential duration of ventricular muscles by activation of ATP-sensitive K^+ channels. *Br. J. Pharmacol.* 115:381–201.

Semb, S. O., and O. M. Sejersted. 1996. Fuzzy space and control of the Na^+,K^+-pump rate in heart and skeletal muscle. *Acta Physiol. Scand.* 156:213–225.

Sperelakis, N. 1995. Electrogenesis of Biopotentials in the Cardiovascular System. Kluwer Academic Publisher, Norwell, MA.

Takano, M., and A. Noma. 1993. The ATP-sensitive K^+ channel. *Prog. Neurobiol.* 41:21–30.

Tani, M., and J. R. Neely. 1989. Role of intracellular Na^+ and Ca^{2+} overload and depressed recovery of ventricular function of reperfused ischemic rat hearts. *Circ. Res.* 65:1045–1056.

Tominaga, M., M. Horie, S. Sasayama, and Y. Okada. 1995. Glibenclamide, an ATP-sensitive K^+ channel blocker, inhibits cardiac cAMP-activated Cl^- conductance. *Circ. Res.* 77:417–423.

Tsuchiya, K., W. Wang, G. Giebisch, and P. A. Welling. 1992. ATP is a coupling modulator of parallel Na,K-ATPase-K-channel activity in the renal proximal tubule. *Proc. Natl. Acad. Sci. U.S.A.* 89:6418–6422.

Tung, P., G. Pai, D. G. Johnson, R. Punzalan, and S. R. Levin. 1990. Relationship between adenylate cyclase and Na^+,K^+-ATPase in rat pancreatic islets. *J. Biol. Chem.* 265:3936–3939.

Urbach, V., E. Van-Kerkhove, D. Maguire, and B. J. Harvey. 1996. Cross-talk between ATP-regulated K^+ channels and Na^+ transport via cellular metabolism in frog skin principal cells. *J. Physiol. (Lond.).* 491:99–109.

Vanheel, B., and A. de Hemptinne. 1992. Influence of KATP channel modulation on net potassium efflux from ischaemic mammalian cardiac tissue. 1992. *Cardiovasc. Res.* 26:1030–1039.

Wendt-Gallitelli, M. F., T. Voigt, and G. Isenberg. 1993. Microheterogeneity of subsarcolemmal sodium gradients: electron probe microanalysis in guinea-pig ventricular myocytes. *J. Physiol. (Lond.).* 472:33–44.